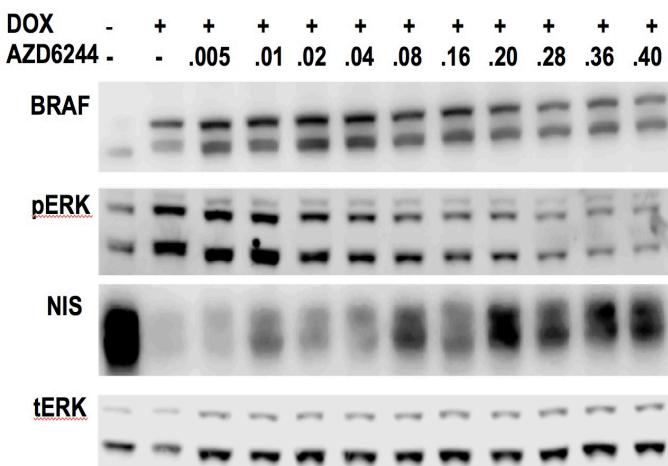
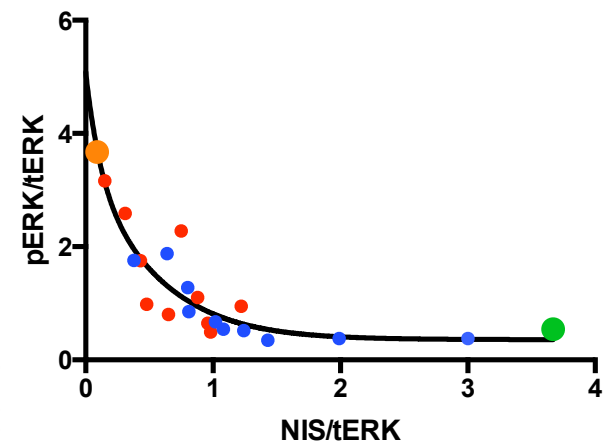
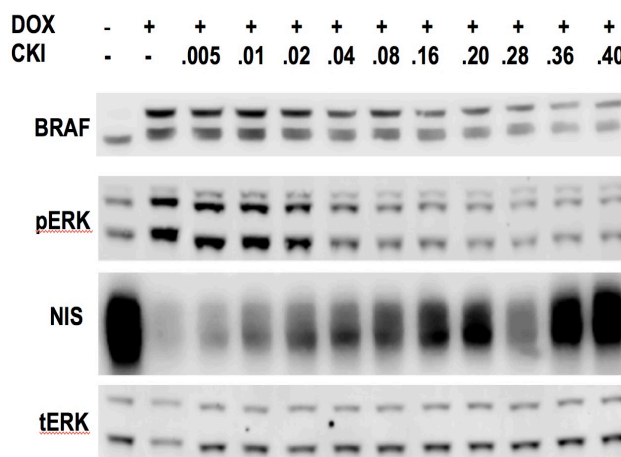


# **Profound blockade of MAPK transcriptional output by combined RAF and MEK inhibition maximizes response to radioiodine therapy in Braf<sup>V600E</sup>-mutant thyroid cancers.**

James Nagarajah<sup>1,2</sup>, Mina Le<sup>1,3</sup>, Jeffrey A. Knauf<sup>1</sup>, Giuseppe Ferrandino<sup>4</sup>, Cristina Montero-Conde<sup>1</sup>, Nagavarakishore Pillarsetty<sup>5</sup>, Alexander Bolaender<sup>5</sup>, Christopher Irwin<sup>2</sup>, Gnana Prakasam Krishnamoorthy<sup>1</sup>, Mahesh Saqcena<sup>1</sup>, Steven M. Larson<sup>2,5</sup>, Alan L Ho<sup>6</sup>, Venkatraman Seshan<sup>7</sup>, Nobuya Ishii<sup>8</sup>, Nancy Carrasco<sup>4</sup>, Neal Rosen<sup>5,6</sup>, Wolfgang A. Weber<sup>2,5</sup> and James A. Fagin<sup>1,6</sup>.

Supplementary Figures and Methods

**A****B**

**Figure S1: Profound inhibition of MAPK signaling is required to restore NIS in thyroid PCCL3-BRAF cells.** **A)** Western blots of PCCL3-BRAF cells treated with dox for 4 days to induce BRAF<sup>V600E</sup>, and then for 3 days with the indicated concentrations AZD6244 or CKI. **B)** Graphs show loading-adjusted pERK vs. NIS levels from the Western blots. Interblot normalization was performed by aligning the – dox and + dox conditions in the two experiments (represented by the large green and orange dots, respectively). Small red and blue dots correspond to experiments in left and right panels of 1A, respectively.

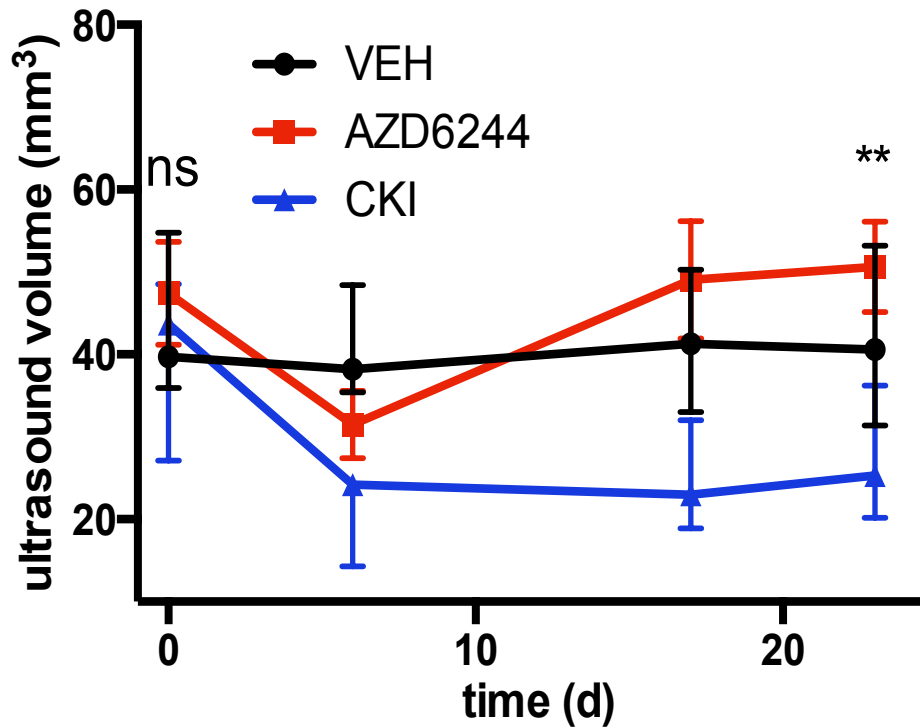


**Figure S2:** Effect of CKI and AZD6244 on thyroid tumor volume of *TPO-Cre/LSL-Braf<sup>V600E</sup>* mice treated for 25 days. Thyroid volume was measured by ultrasound at the indicated times (\*\*p=0.008 for AZD vs. CKI).

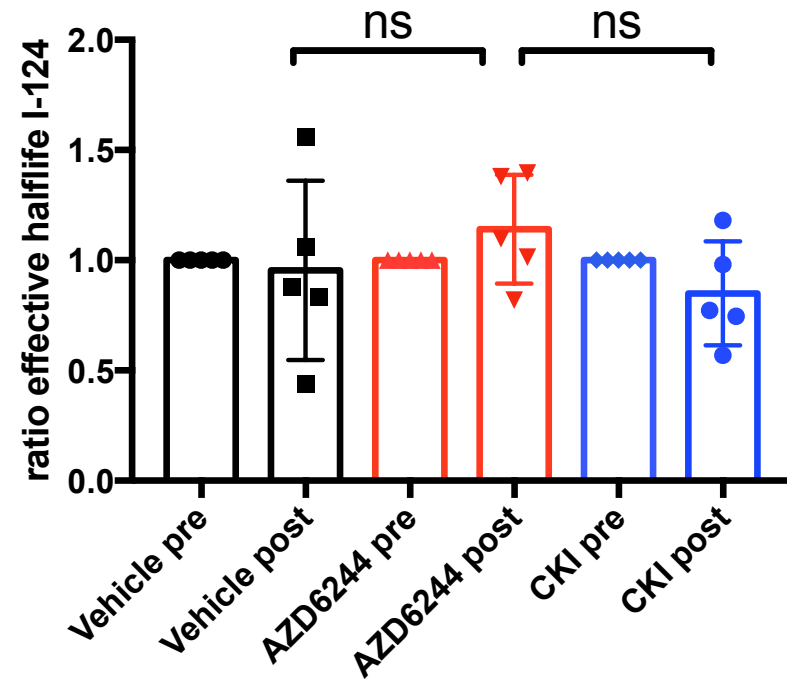
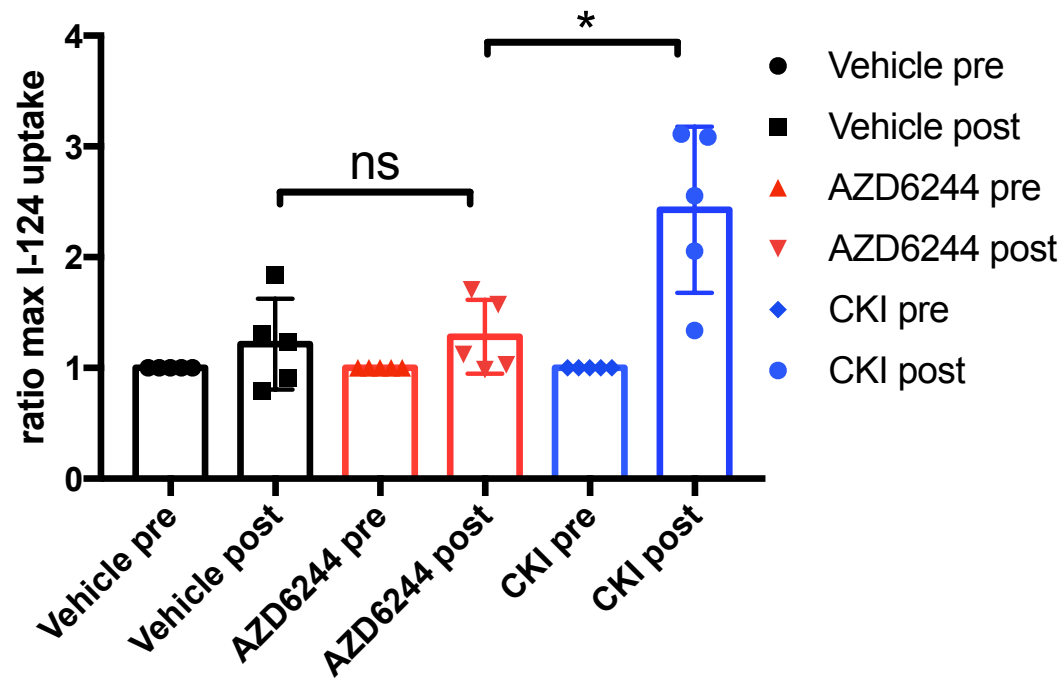


**Figure S3:** *Prolonged treatment with MAPK pathway inhibitors does not further augment iodine uptake nor retention.* I-124 uptake and retention in thyroid tumors was determined with PET/CT before and after 4.5 or 22 days of treatment. The panels show the ratio between the two time points (4.5 vs. 22 days). Iodide uptake and retention was normalized to tumor volume and then used to calculate maximum uptake retention time (mean +/- SD, \*p=0.031 Mann-Whitney test).



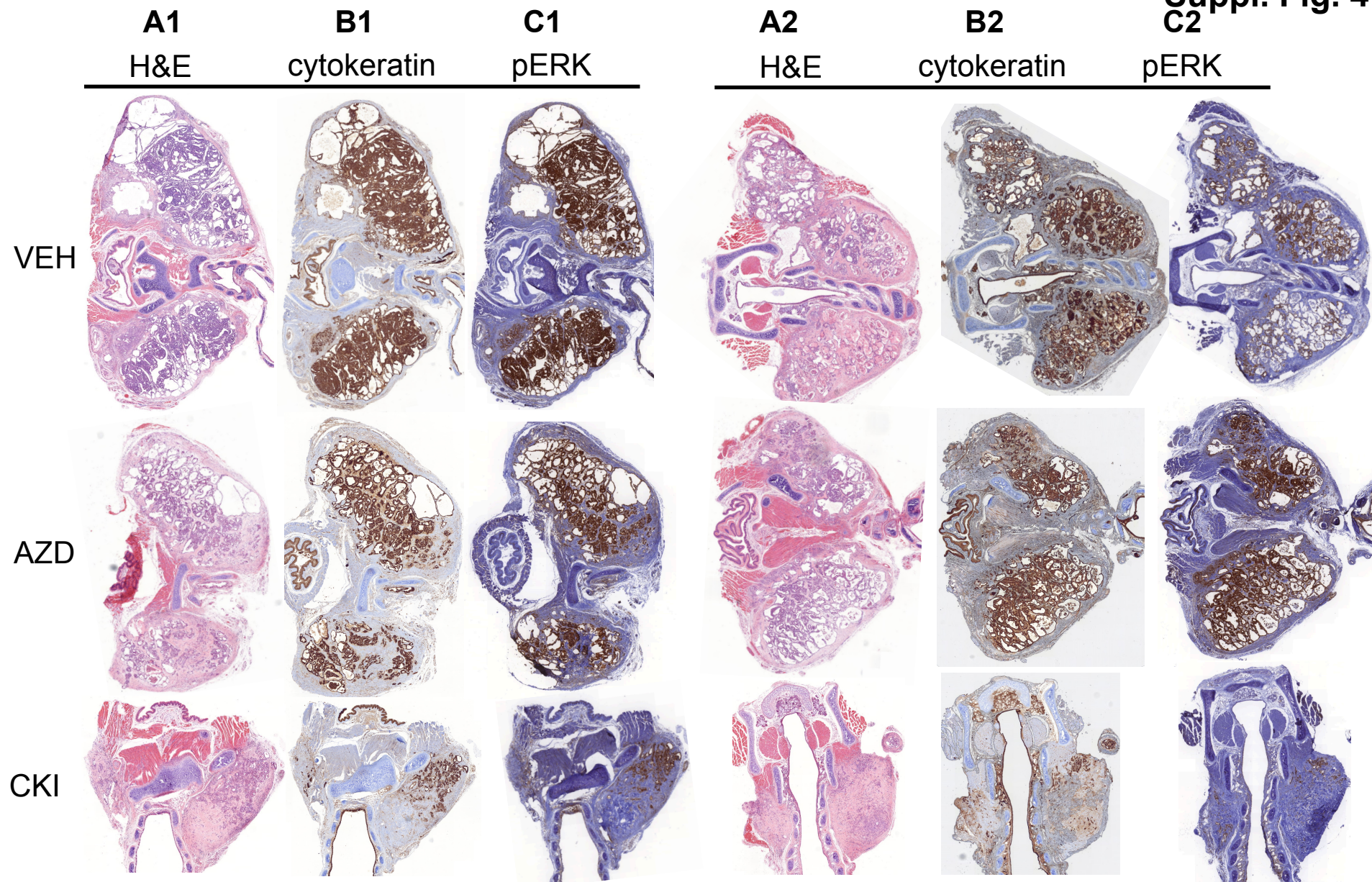


**Figure S4:** Histological characterization of representative sections of thyroid tissues of two additional sets of *TPO-Cre/LSL-Braf<sup>V600E</sup>* mice collected 24 weeks after treatment with vehicle +<sup>131</sup>I, AZD6244 +<sup>131</sup>I or CKI +<sup>131</sup>I. (A1/2) H&E; IHC for pan-cytokeratin (B1/2) or pERK (C1/2).

## Methods:

### Mouse model

Mice with thyroid-specific endogenous expression of *Braf*<sup>V600E</sup> were generated by crossing *TPO-Cre* (1) with *LSL-Braf*<sup>V600E</sup> mice (2), as previously described (3). *TPO-Cre* mice were a gift from Dr. Shioko Kimura (National Cancer Institute, Bethesda, MD), and *LSL-Braf*<sup>V600E</sup> mice were from Dr. Catrin Pritchard (University of Leicester, UK). All experiments were performed on 8-10 weeks old mice. All experiments were approved by the MSKCC IACUC.

### Western blots

PCCL3-BRAF cells (4) or frozen thyroid tissues were lysed in RIPA buffer supplemented with proteinase and phosphatase inhibitors (Roche) and the protein concentration determined using the BCA kit (Thermo Scientific). Western blots were performed on 20 µg protein separated by SDS- PAGE, transferred to PVDF membrane, and immunoblotted using the following primary antibodies: Myc-Tag (#2276S), tERK (#4695S), pERK (#9101L), tMEK (#9122L), p-MEK1/2 (#9121L), all from Cell Signaling Technology or TG (#ab156008) from Abcam. Nancy Carrasco (Yale School of Medicine, New Haven, CT) provided the monoclonal NIS antibody. Proteins were detected either by enhanced chemiluminescence reagents (Pierce) using HRP-conjugated secondary antibodies (Santa Cruz Biotechnology Inc.) or by infrared fluorescence (LI-COR Biosciences), using the appropriate secondary antibody as directed by the manufacturer.

### RNA isolation, cDNA synthesis and qPCR

Total mRNA from snap frozen thyroid tissues was extracted with the PrepEase Kit (USB Corporation). Equal amounts of RNA were reverse transcribed into cDNA using SuperScript® III Reverse Transcriptase (Invitrogen). Quantitative PCR was then performed with the Power SYBR Green PCR Master Mix (Applied Biosystems) with AB-7500 System.  $\beta$ -actin normalized expression was calculated with Q-Gene Core Module (5). Primer sequences are shown in Supplementary Table 1.

### Histology and IHC

Thyroid tissues were immediately placed in 4% paraformaldehyde and incubated overnight at 4°C. The next day, tissue was washed twice with PBS for 30 minutes followed by a single 30-minute 50% ethanol wash. The fixed tissue was then placed in 70% ethanol, paraffin embedded, and sectioned into 4 µm paraffin sections. They were then deparaffinized and immunostained with antibodies for pERK (#9101; Cell Signaling Technology) or pan-cytokeratin (# 760-2135; Ventana) at the Memorial Sloan-Kettering Cancer Center Molecular Cytology Core Facility.

### Serum TSH

A Luminex bead based multiplex assay kit was used for determination of serum

TSH levels according to the manufacturer's protocol (MPTMAG-49K MILLIPLEX xMAP, EMD Millipore).

#### RAI ( $^{124}\text{I}$ -iodide) dosimetry

Imaging was performed using an R4 microPET scanner (Concorde Microsystems) as described (6). Briefly, mice were gavaged with 2.6–3.5 MBq (70–94  $\mu\text{Ci}$ ) of  $\text{Na}^{124}\text{I}$ . Mice were imaged 24 and 72 h later under inhalational isoflurane anesthesia at 1.5 l/min. List-mode data were acquired for 5 minutes using an energy window of 250–750 keV and a coincidence timing window of 6 nsec, histogrammed into 2D projected data by Fourier rebinning, and reconstructed by filtered back-projection using a cut-off frequency equal to the Nyquist frequency. Image visualization and analysis were performed using ASIPro VM software (Concorde Microsystems).

The thyroid volumes pre- and post-treatment were derived from ultrasound imaging (Vevo 2100 micro-ultrasound system VisualSonics, Toronto, Canada), as described (7), and used to calculate the lesion dose per activity as described by Jentzen et al. (8) using the formula:

$$LDpA = \Delta \frac{\int_0^\infty C(t) dt}{Atr \times \rho}$$

where  $C(t)$  was the  $^{131}\text{I}$  activity concentration corrected for the difference in physical half-lives of  $^{124}\text{I}$  (tracer nuclide) and  $^{131}\text{I}$  (therapeutic nuclide),  $\Delta$  the equilibrium  $^{131}\text{I}$  dose constant for nonpenetrating radiation ( $0.11 \text{ Gy g/MBq}^{-1} \text{ h}^{-1}$ ),  $Atr$  the tracer activity shortly after injection, and  $\rho$  the tissue density ( $1 \text{ g/mL}^{-1}$ ).

#### RAI therapy ( $^{131}\text{I}$ ):

Preparation, dilution, and injection of  $^{131}\text{I}$ -Nal were performed in a designated Comecer (Castelle Bolognese) radioisotope fume hood. Approximately 37 MBq (1 mCi) of USP-grade  $^{131}\text{I}$ -Nal (Nuclear Diagnostic Products) in 100–200  $\mu\text{l}$  isotonic saline was administered to each mouse via gavage. Mice were placed in a designated radioactive animal holding facility. The 1 mCi dose was selected to achieve a response in the drug-treated groups according to dose-response calculations estimated as previously described (9, 10).

#### $^{18}\text{F}$ -TFB PET imaging:

$^{18}\text{F}$ -TFB synthesis was performed as described (11). Mice were injected with  $\sim 120 \mu\text{Ci}$   $^{18}\text{F}$ -TFB intraperitoneally and PET images acquired for 30 minutes after injection using the same R4 microPET scanner and technique used for  $^{124}\text{I}$ -PET with an energy window of 450–650 keV. PET scans were performed prior to and on 1, 2, 4, 9, 12 and 23 days after drug treatment. Thyroid tissue volumes were derived from ultrasound imaging performed prior to and 6, 17 and 23 after starting drug therapy. TFB uptake was calculated as described for  $^{124}\text{I}$ -PET.

#### <sup>18</sup>F-TFB kinetics:

Rat small intestinal IEC-6 cells (purchased from American Type Culture Collection, Manassas, VA) were washed twice with Hanks' balanced salt solution (HBSS) [140 mM NaCl, 5.4 mM KCl, 1.3 mM CaCl<sub>2</sub>, 0.4 mM MgSO<sub>4</sub>, 0.5 mM MgCl<sub>2</sub>, 0.4 mM Na<sub>2</sub>HPO<sub>4</sub>, 0.44 mM KH<sub>2</sub>PO<sub>4</sub>, 5.55 mM glucose and 10 mM HEPES (pH 7.5)]. For steady-state experiments, cells were incubated with HBSS containing 3 or 50 μM TFB supplemented with <sup>18</sup>F-TFB. Incubations proceeded at room temperature for 30 min. For TFB-dependent kinetic analysis, cells were incubated in HBSS buffer containing the indicated TFB concentrations (0.23– 40 μM) for 2 min.

Accumulated <sup>18</sup>F-TFB was released with ice-cold ethanol and then quantified in a Beta-counter (PerkinElmer, USA). DNA concentration was determined by the diphenylamine method after trichloroacetic acid precipitation (12). Iodide uptake was expressed as pmol/μg DNA. Initial-rate data were analyzed by non-linear regression using the following equation:  $v = (V_{max} * [I]) / (K_m + [I])$ . Background obtained in absence of Na<sup>+</sup>, while keeping the medium isotonic with choline chloride, was subtracted. Data were analyzed with Origin 9 ([www.originlab.com](http://www.originlab.com)).

#### Statistical Analysis

The statistical software GraphPad-Prism (version 6.0; GraphPad Software, Inc. CA, USA) was used to analyze the data. All reported p-values were calculated using the two-sided Mann-Whitney Test or Wilcoxon Signed Rank Test as indicated in the legends, and a p-value of <0.05 was considered significant. All data are represented as mean +/- SEM unless otherwise indicated.

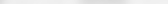


## Reference List

1. Kusakabe, T., Kawaguchi, A., Kawaguchi, R., Feigenbaum, L., and Kimura, S. 2004. Thyrocyte-specific expression of Cre recombinase in transgenic mice. *Genesis* 39:212-216.
2. Mercer, K., Giblett, S., Green, S., Lloyd, D., DaRocha Dias, S., Plumb, M., Marais, R., and Pritchard, C. 2005. Expression of endogenous oncogenic V600EB-raf induces proliferation and developmental defects in mice and transformation of primary fibroblasts. *Cancer Res* 65:11493-11500.
3. Franco, A.T., Malaguarnera, R., Refetoff, S., Liao, X.H., Lundsmith, E., Kimura, S., Pritchard, C., Marais, R., Davies, T.F., Weinstein, L.S., et al. 2011. Thyrotrophin receptor signaling dependence of Braf-induced thyroid tumor initiation in mice. *Proc Natl Acad Sci U S A* 108:1615-1620.
4. Mitsutake, N., Knauf, J.A., Mitsutake, S., Mesa, C., Jr., Zhang, L., and Fagin, J.A. 2005. Conditional BRAFV600E expression induces DNA synthesis, apoptosis, dedifferentiation, and chromosomal instability in thyroid PCCL3 cells. *Cancer Res* 65:2465-2473.
5. Muller, P.Y., Janovjak, H., Miserez, A.R., and Dobbie, Z. 2002. Processing of gene expression data generated by quantitative real-time RT-PCR. *Biotechniques* 32:1372-1374, 1376, 1378-1379.
6. Chakravarty, D., Santos, E., Ryder, M., Knauf, J.A., Liao, X.H., West, B.L., Bollag, G., Kolesnick, R., Thin, T.H., Rosen, N., et al. 2011. Small-molecule MAPK inhibitors restore radioiodine incorporation in mouse thyroid cancers with conditional BRAF activation. *J Clin Invest* 121:4700-4711.
7. Garcia-Rendueles, M.E., Ricarte-Filho, J.C., Untch, B.R., Landa, I., Knauf, J.A., Voza, F., Smith, V.E., Ganly, I., Taylor, B.S., Persaud, Y., et al. 2015. NF2 Loss Promotes Oncogenic RAS-Induced Thyroid Cancers via YAP-Dependent Transactivation of RAS Proteins and Sensitizes Them to MEK Inhibition. *Cancer Discov* 5:1178-1193.
8. Jentzen, W., Freudenberg, L., Eising, E.G., Sonnenschein, W., Knust, J., and Bockisch, A. 2008. Optimized 124I PET dosimetry protocol for radioiodine therapy of differentiated thyroid cancer. *J Nucl Med* 49:1017-1023.

9. Maxon, H.R., 3rd, Englaro, E.E., Thomas, S.R., Hertzberg, V.S., Hinnefeld, J.D., Chen, L.S., Smith, H., Cummings, D., and Aden, M.D. 1992. Radioiodine-131 therapy for well-differentiated thyroid cancer--a quantitative radiation dosimetric approach: outcome and validation in 85 patients. *J Nucl Med* 33:1132-1136.
10. Jentzen, W., Hoppenbrouwers, J., van Leeuwen, P., van der Velden, D., van de Kolk, R., Poeppel, T.D., Nagarajah, J., Brandau, W., Bockisch, A., and Rosenbaum-Krumme, S. 2014. Assessment of lesion response in the initial radioiodine treatment of differentiated thyroid cancer using 124I PET imaging. *J Nucl Med* 55:1759-1765.
11. Jauregui-Osoro, M., Sunassee, K., Weeks, A.J., Berry, D.J., Paul, R.L., Cleij, M., Banga, J.P., O'Doherty, M.J., Marsden, P.K., Clarke, S.E., et al. 2010. Synthesis and biological evaluation of [(18)F]tetrafluoroborate: a PET imaging agent for thyroid disease and reporter gene imaging of the sodium/iodide symporter. *Eur J Nucl Med Mol Imaging* 37:2108-2116.
12. Nicola, J.P., Basquin, C., Portulano, C., Reyna-Neyra, A., Paroder, M., and Carrasco, N. 2009. The Na<sup>+</sup>/I<sup>-</sup> symporter mediates active iodide uptake in the intestine. *Am J Physiol Cell Physiol* 296:C654-662.

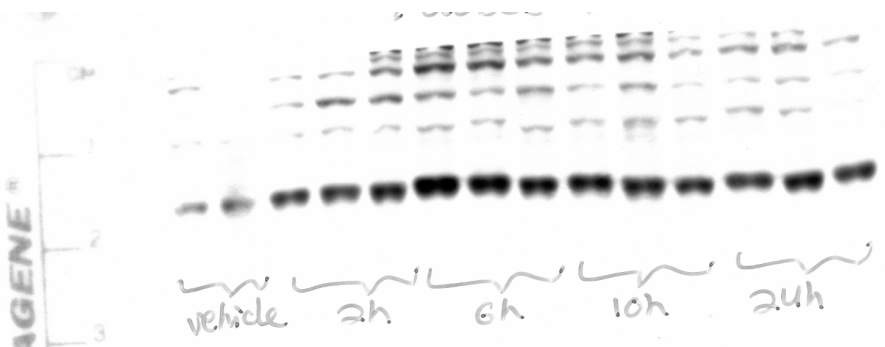
## The image displays two separate gel electrophoresis results. The top gel consists of 10 lanes, each showing a series of horizontal bands at different molecular weights. The bottom gel also consists of 10 lanes, but each lane features a single, very prominent and thick horizontal band, suggesting a high concentration of a specific DNA fragment or a different experimental condition.



\_\_\_\_\_

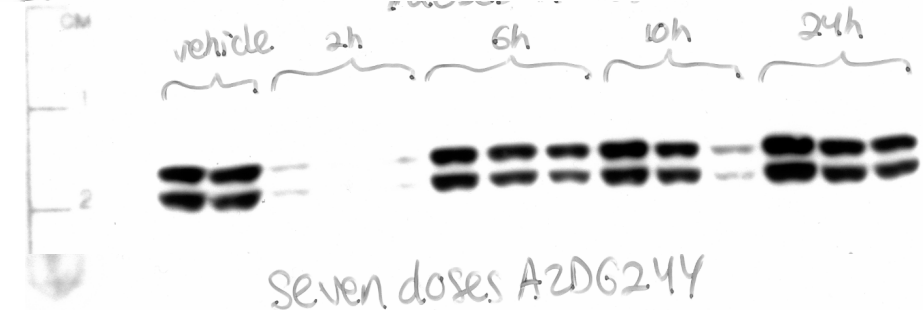
Scanned films for Figure 1 C

pMEK



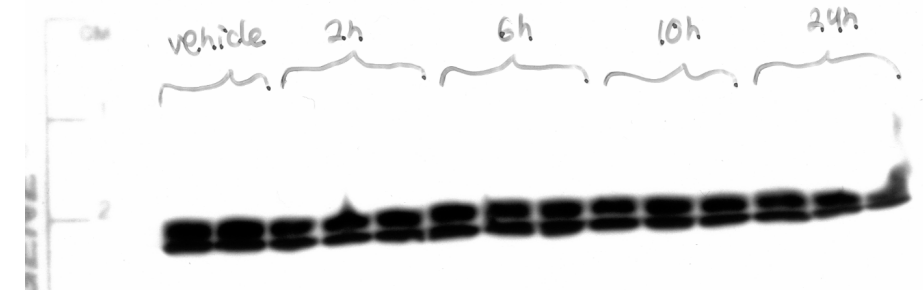
pMEK

pERK



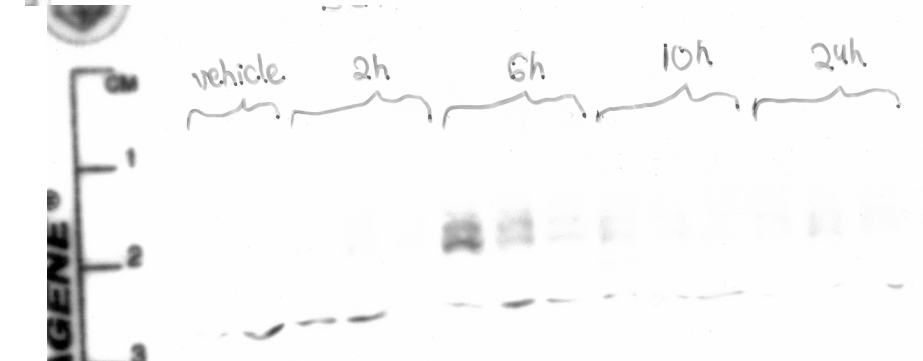
pERK

tERK



tERK

Nis

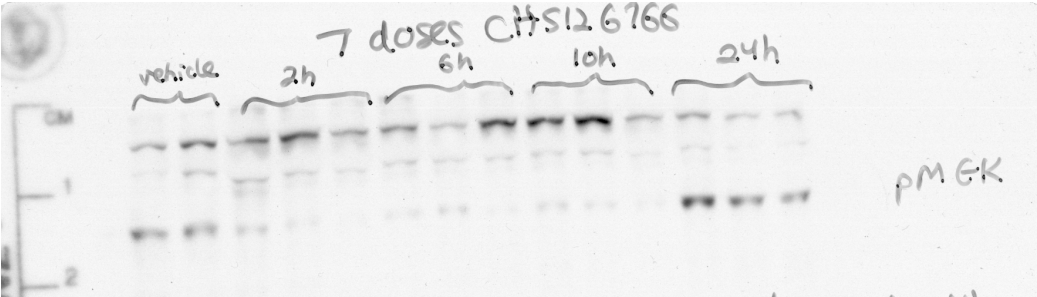


NIS

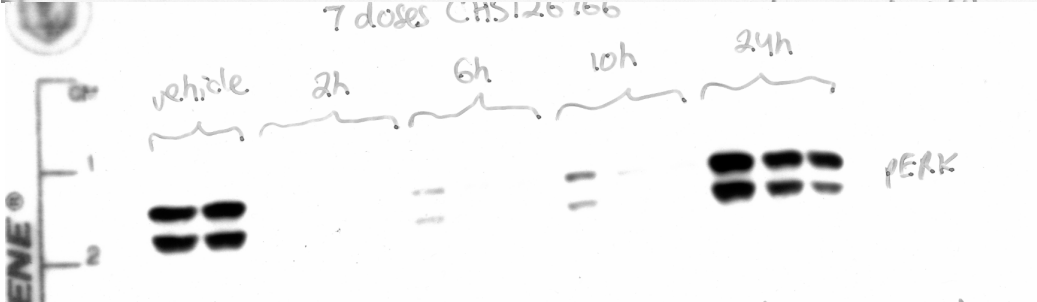


Scanned films for Figure 1 D

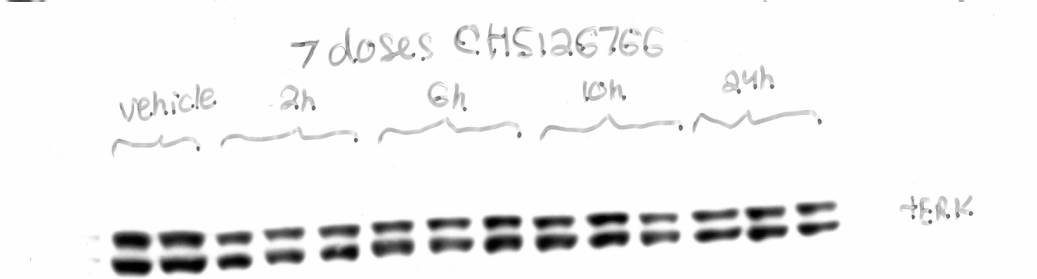
pMEK



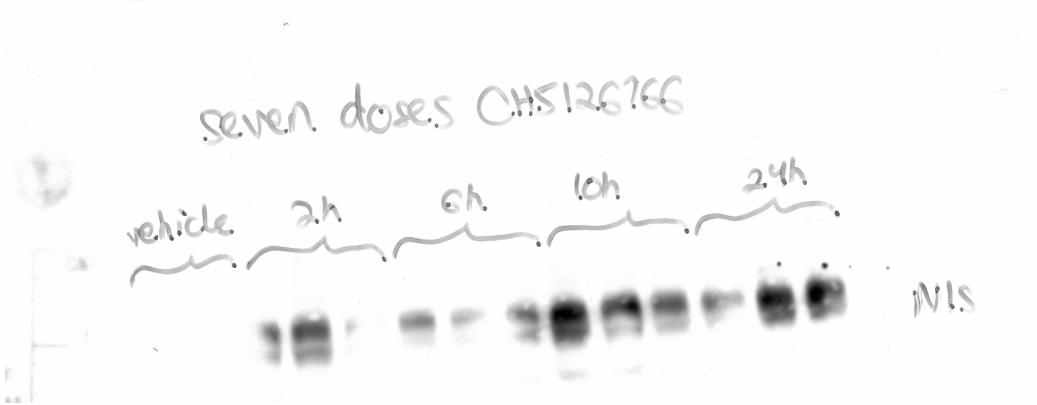
pERK



tERK



Nis



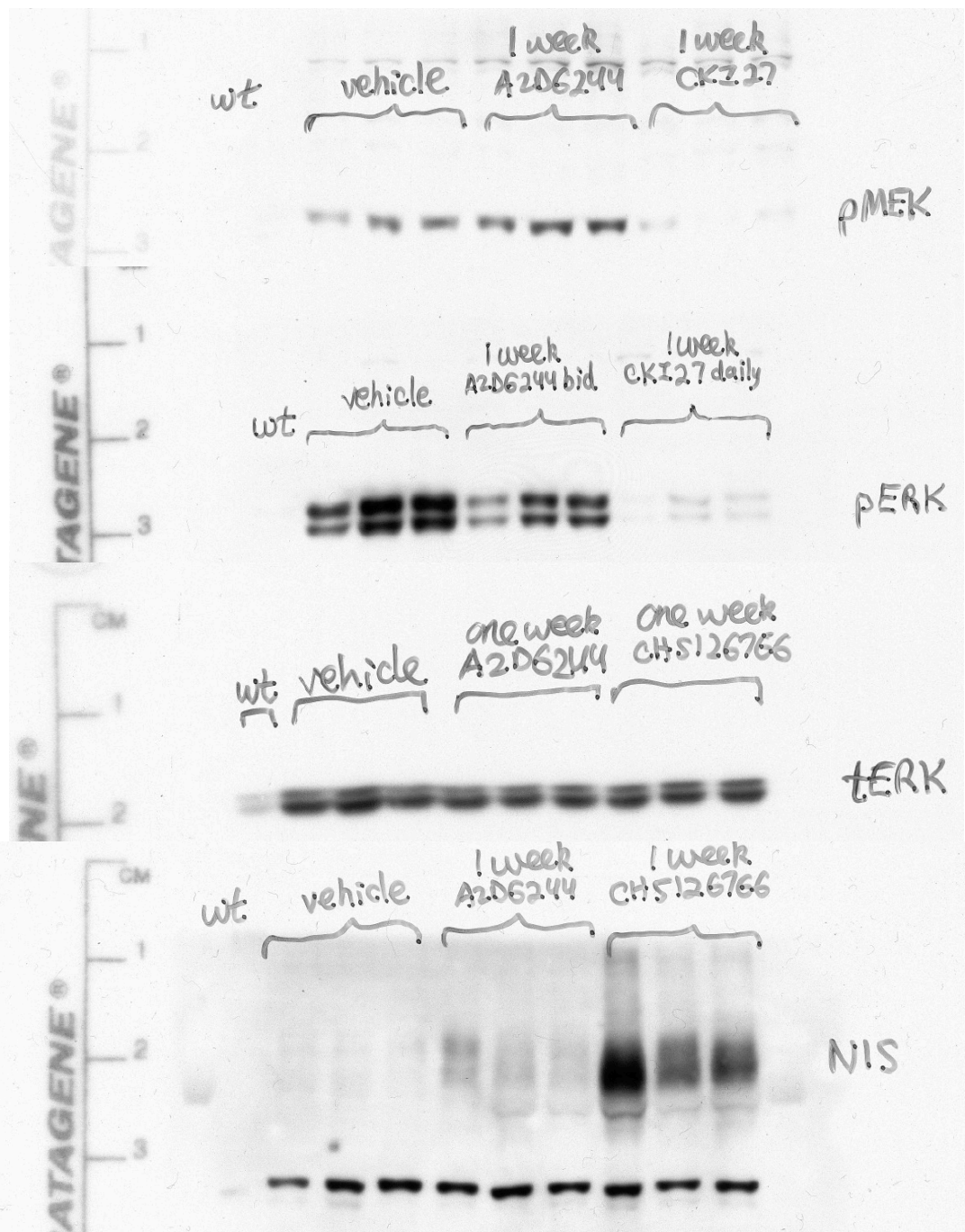
Scanned films for Figure 1 E  
(lanes 2-9 were used for manuscript)

pMEK

pERK

tERK

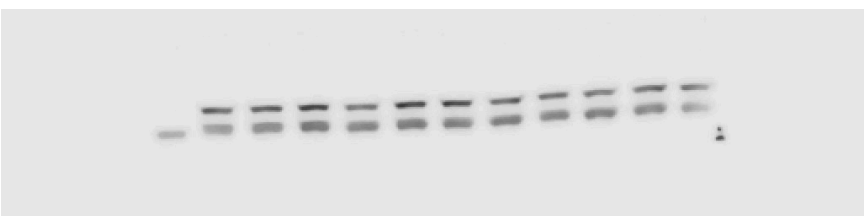
Nis



# Suppl. Figure 1

(lanes 1-12 were used for manuscript)

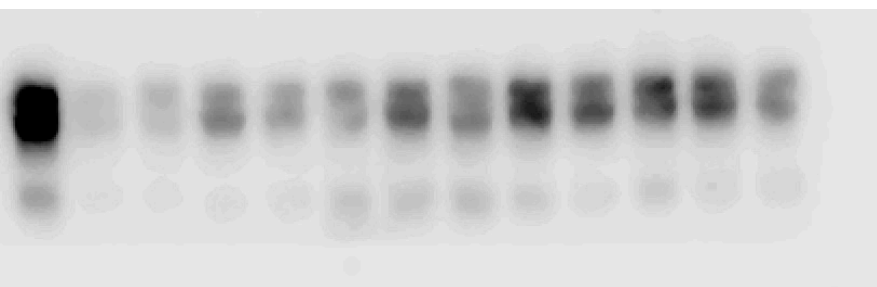
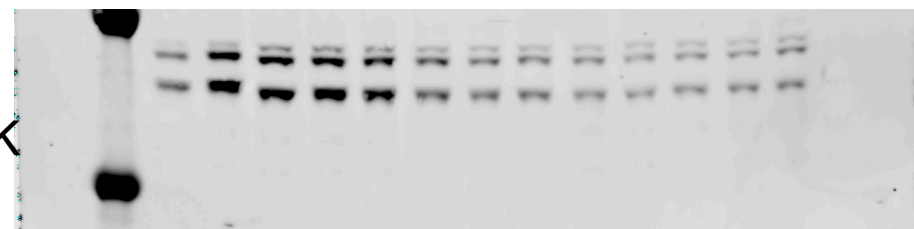
Licor was used for p/t ERK. Camera captured bands for Nis)



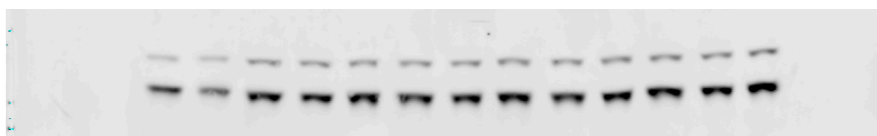
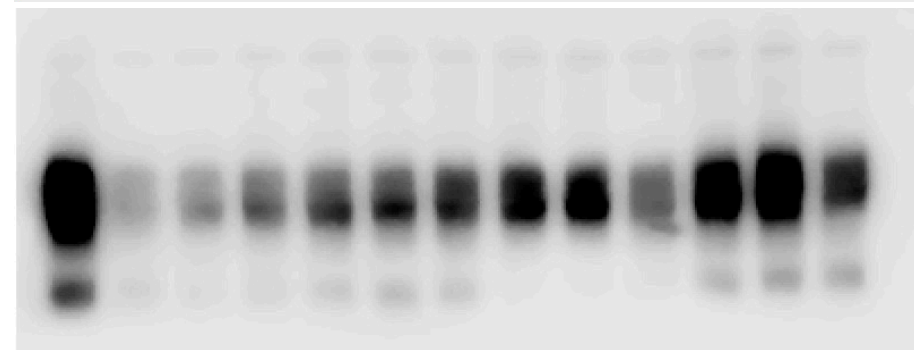
BRAF



pERK



Nis



tERK

